International Journal of Geosynthetics and Ground Engineering (2020) 6:56
https://doi.org/10.1007/s40891-020-00240-z

ORIGINAL PAPER

Numerical Evaluation of Buried Wave Barriers Performance

A. Moussa[1] · **Hany El Naggar**[1]

Received: 15 September 2020 / Accepted: 2 November 2020 / Published online: 21 November 2020

Abstract
Ground-borne vibrations caused by construction activities, highway and railway traffic may disturb adjacent structures and sensitive machines. Thus, studies on isolation of this type of vibrations have accelerated in recent years. This paper aims to develop a plain strain 2D finite element model (FEM) to investigate the use of open and buried trenches in mitigating the unfavorable vibrations from a concrete machine foundation subjected to sinusoidal harmonic load. The finite element model is validated using a conducted filed test on open and infilled trenches. Then, the FEM model was used to conduct a parametric study to investigate the effect of the barrier depth and buried depth on the screening effectiveness of the buried infilled trenches. Special cases, i.e., buried dual and trapezoidal trenches, were also considered to improve the effectiveness of infilled buried trenches. The results of this study show that the open trench is the optimum wave barrier and increasing the burial depth would lead to a significant reduction in the screening effectiveness of buried trenches. However, buried trapezoidal trenches could significantly increase the performance of buried trenches by 20% compared to a single rectangular buried trench. Similarly, double buried trenches improved the mitigation capacity of buried trenches by 25% compared to a single rectangular buried trench.

Keywords Buried trenches · Vibration screening · Infilled trenches · Wave propagation · FEM

Introduction

There are a number of man-made activities that could generate undue ground vibrations such as vibrating machines, traffic and construction activities. These vibrations propagate through the soil medium and could damage the adjacent structures or sensitive machines. Furthermore, if these vibrations are generated frequently in residential areas, it will become a source of continuous annoyance to the residents. Thus, vibration isolation is a very important matter to be addressed. To reduce the propagation of the undesired vibrations to the nearby structures or machines, a barrier could be constructed across the propagation path of the surface waves. The barrier is a geometric or material discontinuity in the half space soil medium, which intercepts the propagated vibrations and reduce their amplitude, [1]. The trench barriers are used in two cases to mitigate the waves propagations: (a) active or near field isolation where the barrier is placed near from the vibration source and (b) passive or far field isolation, where the trench is placed far from the vibration source and near from the structure or machine that to be protected. There are several types of barriers such as trenches (open or infilled), sheet piles, a row of solid or tubular piles, concrete walls, diaphragm walls, gas-cushion screen, etc., [2].

Vibration sources creates two types of vibrations that depend on the way of propagation in soil, i.e., continuous and transient vibrations. Activities such as pile driving or traffic cause continuous vibrations, while blasting or dropping impact hammer cause transient vibrations. The vibration isolation problems are mainly caused by the continuous sources. Construction activities and traffic could induce vibrations that have peak velocity and frequency of 1–50 mm/s and 10–60 Hz, respectively [3]. Furthermore, trains could generate vibrations that have a peak velocity larger than 100 mm/s. However, only a peak velocity of 2.5 mm/s is very enough to be perceived by humans. Thus, screening the vibrations of larger amplitudes is of a paramount importance, especially in the urban areas.

✉ Hany El Naggar
hany.elnaggar@dal.ca

A. Moussa
ahmed.moussa@dal.ca

[1] Department of Civil and Resource Engineering, Dalhousie University, Halifax, NS B3H 4R2, Canada

Barkan [4] has been the first to utilize open trench as wave barrier. Open trench and sheet pile couple were employed to mitigate vibration generated by traffic, a system that proved to be inadequate. Then, the efficiency of solitarily open trench was evaluated through Woods [5] field experiments. The vibration generator comprised a vertically oscillating vibration exciter on a circular footing. The author considered circular trenches of multiple geometric characteristics to examine the efficacy of open trenches in isolating vibrations. Active isolation required the trench depth to be at least 0.6 of the wave length (L_r), whereas passive isolation required a depth of 1.19 L_r. Jesmani et al. [6], on the other hand, conducted 3D finite element studies on deep foundation isolation using open trench. The authors show that a trench depth of at least half the length of the pile is necessary for a satisfactory performance. Finite element analysis was also employed by Çelebi and Kırtel [7] to examine the impact of train-induced vibrations on the soil–structure interaction. The results indicate that open trenches minimized vertical vibration by 85%. Since instability issues could associate with open trenches because of the soil stiffness, infilled trenches were used to preserve the trench stability. The impact of EPS wave barriers on traffic loading vibrations was studied by Murillo et al. [8] through centrifuge tests. It has been pointed out that the dimensions of the geofoam barrier must be carefully selected. For instance, the depth and width of the EPS geofoam barrier must be larger than $0.25\lambda_R$ and $1.5\lambda_R$, respectively. FLAC finite difference program has been employed by Orehov et al. [9] to evaluate the screening efficiency of water barriers. The results report a significant reduction in soil particle displacement when water barriers are deployed. In multiple works, Haupt [10–12] varied the geometric configuration of rectangular concrete walls and investigated the resulting effects on the vibration isolation of these barriers. Haupt [11] concludes that the appropriate selection of the barrier's cross-sectional area is crucial for efficient isolation. However, El Naggar and Chehab [13] reported that soft barriers can surpass concrete-filled trenches. Moreover, rubber chip barriers have been studied by Zoccali et al. [14] through finite element analysis. The former modeled rubber chip barrier in elastic half space through ADINA finite element software. Despite the high damping ability of the rubber chip, its isolation performance reported to be unsatisfactory. The latter, however, examined the isolation performance of rubber chip filled wave barriers through 3D finite element analysis. The results showed that the peak particle velocity has been decreased by only 5%.

Yarmohammadi et al. [15] conducted an extensive parametric study to develop a coupled genetic algorithm/finite element methodology for the design of wave barriers. Several critical factors were considered in developing the newly proposed methodology such as trench shape, dimensions, dual–triple trench systems, and material properties of infilled trenches. The authors considered in their evaluation the trapezoidal trenches which are not covered in details in the literature. It was concluded that the rectangular and semi-circular trenches have the highest and lowest performance, respectively. The optimum type of trench barriers is the open trenches, especially if a double trench system has been used. Additionally, the trench depth and width are the highest and lowest factors, respectively, that influence the trench performance. Furthermore, a similar innovative methodology was developed by Yarmohammadi and Rafiee-Dehkharghani [16] to find the optimal design procedure of trench barriers to mitigate the underground and above-ground railway vibrations. Three wave barriers were considered in the designing procedure, namely wave impeding blocks (WIBs), jet-grouted columns and trenches. It was also concluded that open trenches significantly outperformed the WIBs and jet-grouted columns wave barriers. Nevertheless, if the installation of open trenches was not applicable, WIBs were recommend to be used more than jet-grouted columns due to its better performance.

The aforementioned research was focused on the performance evaluation of open or infilled trench barriers. However, for several practical reasons, open or infilled trenches could be covered by soil. These reasons could include reconstruction, safety or greenery. In this regard, Feng et al. [17] investigated the buried trenches performance in vibration screening. The authors developed 2D axisymmetric FEM to assess the performance of a buried concrete trench. The vibration source was modeled as a sinusoidal harmonic load with a magnitude of 1 kN and a frequency of 30 Hz. It was concluded that the trench depth and buried depth are the main parameters that control the buried trenches effectiveness in vibration screening; whereas, the effect of buried trench depth is relatively minimal.

The aim of this paper is to provide more insights on the various parameters that affect the performance of buried trenches which are used to mitigate the propagating vibrations from a machine foundation. Furthermore, a parametric study is conducted to investigate the most significant factors that affect the performance of trench wave barriers which are the depth of the trench, the source frequency, the infilled material and the shear wave of the soil. In addition, to the best of the authors' knowledge, the investigation of the effectiveness of trapezoidal-shaped vibration barriers in the literature is limited; thus, it is deemed necessary to evaluate the screening efficiency of buried trapezoidal trenches. Lastly, the performance of a dual trench system is evaluated and compared with the performance of the single trench system.

Model Development

Problem Definition

The problem of rigid embedded strip machine foundation subjected to sinusoidal harmonic load resting on sandy soil has been considered in this work. The width of the concrete foundation is considered to be 1 m and its thickness is 0.5 m. It was assumed that the machine operating frequency (f) is 10 Hz with a load amplitude (P_o) of 5 kN/m^2. Furthermore, the estimated machine weight and other accessories were 10 kN/m^2. The material properties for the soil deposit and concrete footing are presented in Table 1. The damping of the concrete material of the footing was not considered to ensure that all vibrations are propagated into the soil without affecting its amplitude. To avoid the dependency on the frequency of the vibration source, the trench depth (d), trench width (w), burial depth (h) and the distance from the vibration source to the trench (l) were normalized by the Rayleigh wavelength (λ_R), as shown in Fig. 1. Based on Eqs. 1 and 2, the calculated λ_R is equal to 7.8 m. The normalized trench width (W) and the normalized distance from the vibration source to the trench (L) are equal to $0.07\lambda_R$ and $0.4\lambda_R$, respectively, throughout the study.

Table 1 Material properties of the soil deposit and concrete footing

Soil parameters	Notations	Soil	Concrete footing
Unit weight	ρ	18.5 kN/m^3	23.5 kN/m^3
Elastic modulus	E	35 MPa	25 GPa
Poisson's ratio	ν	0.32	0.15
Shear wave velocity	V_s	83.85 m/s	2130 m/s
Damping	ξ	5%	–

$$V_R = \left(\frac{0.87 + 1.12}{1 + \nu}\right) V_s, \tag{1}$$

$$\lambda_R = {}^{V_R}/_{f}. \tag{2}$$

The effectiveness of buried trenches barriers is evaluated in terms of amplitude reduction factor (A_R) over a specified distance behind the trench barrier as defined by Woods [5]. In this study, the A_R ratios were calculated up to a distance of $4\lambda_R$ behind the trench barrier. However, the A_R values are not uniform over the range of 4λ; thus, the overall degree of isolation is in terms of average amplitude reduction ratio (AA_R) which is the weighted average of the amplitude reduction ratios obtained over the specified range of study (i.e., 4λ). The A_R and AA_R are calculated using Eqs. 3 and 4.

$$A_R = \frac{\text{maximum displacement amplitude after the trench}}{\text{maximum displacement amplitude before the trench}}, \tag{3}$$

$$AA_R = \frac{1}{4\lambda_R} \int_0^{4\lambda_R} A_R(x)\mathrm{d}x. \tag{4}$$

Development of the FE Model

A 2D plain strain model was developed using the finite element software PLAXIS 2D to simulate the considered problem. 15-Noded element was employed in building the model. In PLAXIS 2D, the sinusoidal dynamic load is defined by Eq. 5.

$$P_{(t)} = P_o \sin(\omega t + \emptyset), \tag{5}$$

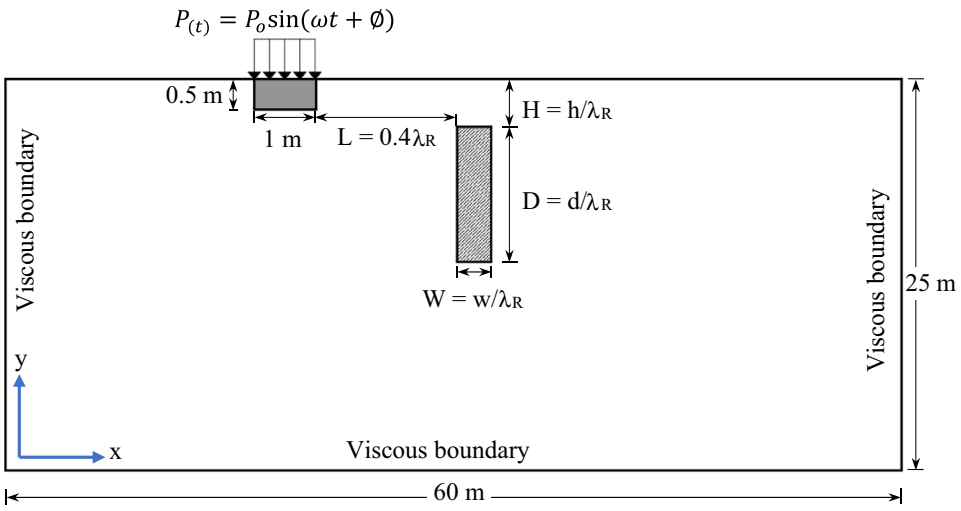

Fig. 1 A schematic diagram for the considered problem

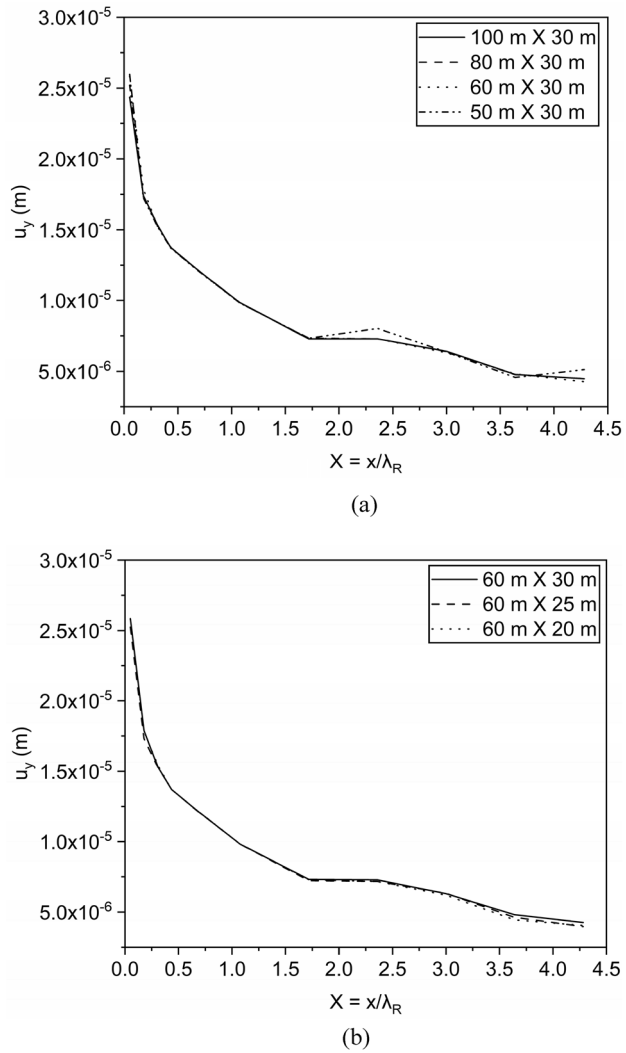

Fig. 2 Convergence analysis of model dimensions: **a** model width, **b** model height

where P_o is the amplitude of the harmonic load, ω is the angular frequency and equal to $2\pi f$ and $\varnothing$ is the initial phase angle in degrees.

In addition, the width and height of the numerical model were selected to be 60 m and 25 m, respectively. The selected width and height of the developed model were selected based on the convergence analysis shown in Fig. 2. The vertical displacement was monitored at various points away from the vibration source. As shown from Fig. 2a, at a model width less than 60 m, significant variation in the monitored displacements is observed especially after a normalized distance from the vibration source (X) equal to 2. Thus, a model width equal to 60 m was considered. Furthermore, the model height was then investigated as shown in Fig. 2b. Varying the model height did not affect the measured vertical displacement significantly. Therefore, a model height equal to 25 m was considered.

Figure 3 shows the generated mesh for the considered problem. Two mesh zones were employed in the developed model; the zone near from the concrete footing and the buried trench which has an average element size of 0.195 m, while the second zone has an average element size of 0.92 m. As recommended by Kramer [18], zone two average element size was less than one-eighth the Rayleigh wavelength (λ_R); however, the average element size of zone one was less than one-tenth the Rayleigh wavelength (λ_R). This meshing technique was employed to improve the accuracy of the developed model without adding excessive computational time.

The soil deposit, the concrete footing and the infilled material are modeled using linear elastic model. In general, soil behaves linearly at shear strain levels below or equal to 10^{-3}%, Kramer [18]. However, at a higher shear strain amplitude, the soil nonlinearity should be considered. In this study, the static loads, i.e., machine self-weight, and the

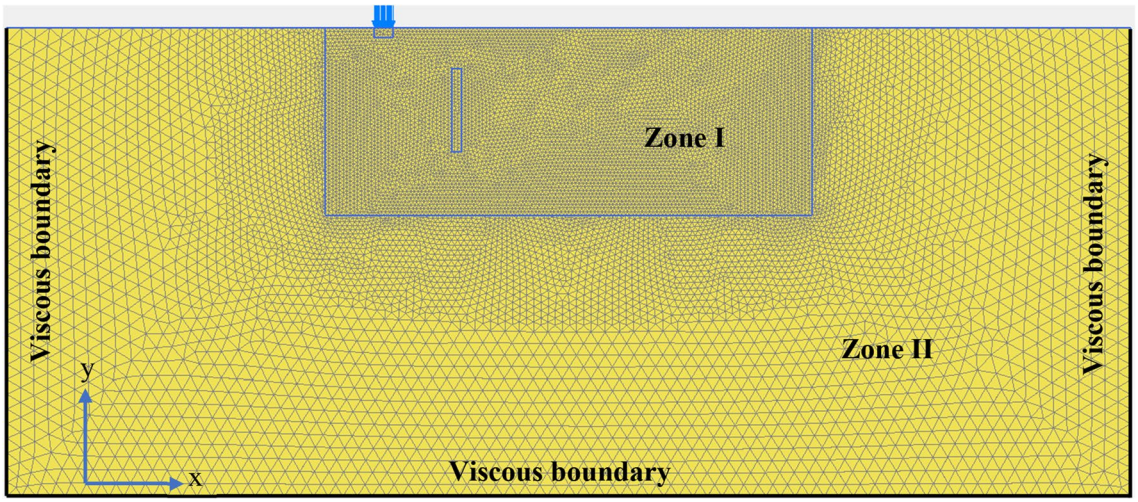

Fig. 3 Generated mesh for the developed numerical model

dynamic load amplitude (P_o) did not develop shear strain levels above 10^{-3}% within the soil medium. Hence, it was reasonable to adopt the linear elastic model.

Furthermore, the model left and right boundaries were restrained from the movement in the horizontal direction and only allowed to move in the vertical direction. Whereas, the model bottom boundary was fully restrained in both directions. Moreover, as shown in Fig. 3, viscous boundaries were employed to avoid the spurious wave reflections near to the model boundaries. PLAXIS 2D adopt the dampers proposed by Lysmer and Kuhlemeyer [19] for the viscous boundary conditions. The dampening of the normal (σ_n) and shear stress (τ_s) are given by the following equations:

$$\sigma_n = -C_1 \rho V_p \dot{u}_x, \tag{6}$$

$$\tau_s = -C_2 \rho V_s \dot{u}_y, \tag{7}$$

where C_1 and C_2 are the wave relaxation coefficients; V_p and V_s are the pressure and shear waves, respectively; $\dot{u}_x$ and $\dot{u}_y$ are the particle velocities in the normal and tangential directions of the boundaries, respectively.

The wave relaxation coefficient (C_1) improves the damping of the body waves in the normal direction to the model boundary; while, the wave relaxation coefficient (C_2) improves the dampening of the shear waves in the tangential direction to the model boundary. Brinkgreve and Vermeer [20] and Wang et al. [21] recommended the use of $C_1 = 1$ and $C_2 = 0.25$ to achieve a reasonable wave absorption at the model boundaries. Thus, in this study, the same values were considered for C_1 and C_2.

A total of dynamic analysis time of 3 s was considered to ensure the propagation of Rayleigh waves throughout the model. The dynamic time step (Δt) was calculated based the smallest element size (I_{min}) in the finite element model. According to Eq. (8), the critical time step ($\Delta t_{critical}$) was equal to 1.4×10^{-3}; hence, to ensure the accuracy of the numerical modeling, the dynamic time step (Δt) used in this study was 5×10^{-4}.

$$\Delta t \leq \Delta t_{critical} = \frac{I_{min}}{V_s}. \tag{8}$$

Model Validation

Case I: Alzawi and El Naggar [1]

Alzawi and El Naggar [22] conducted a full-scale experimental test on the vibration screening using open and geofoam-infilled trenches. The trench geometry was 20 m long, 0.25 m wide and 3 m deep. Figure 4 shows the plan layout of the considered experimental field test. As shown in Fig. 4, 24 one-directional geophones were used to measure the vertical velocity induced in the soil. All geophones were placed 2.5 m apart from each other along the center line of the trench. The excitation source used was a mechanical oscillator that is capable of generating a sinusoidal force of 23.5 kN peak to peak with a frequency range of 4–40 Hz. The distance from the trench to the excitation source varied to investigate its effect on the performance on open and geofoam trenches, as indicated in Fig. 4. In this paper, only the field test results related to the 1st location and exciting frequency of 40 Hz were used to validate the developed FEM. The soil was modeled as a linear elastic material. The soil unit weight (γ), Poisson's ratio (ν), soil damping (ξ) and shear wave velocity (V_s) are 18.7 kN/m^3, 0.4, 5% and 225 m/s, respectively.

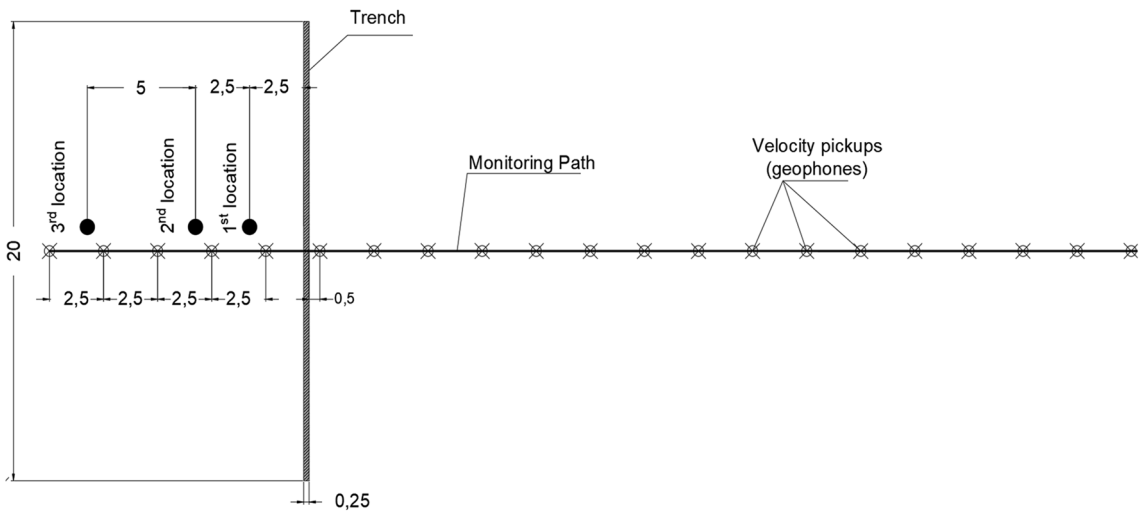

Fig. 4 Field test layout and geophones numbering and locations, Alzawi and El Naggar

Figure 5 a, b shows the obtained maximum vertical velocity (v_y) from the FEMs for the no trench and open trench models versus the normalized distance to the source (X). By comparing the obtained results with the field test results, it could be observed that the developed 2D FEMs are capable of reasonably predicting the trend of the reduction in vibrations amplitudes. However, the variation between the obtained values from the finite element models and the field test for both models is mainly due to the assumption that the problem at hand could be numerically solved as a 2D plain strain problem. In addition, the material model used, i.e., linear elastic model, is incapable to produce better prediction for the soil vertical velocities because the native soil at the field is not homogeneous and definitely not purely elastic. This difference between the obtained values of the FEMs and the field test results is clearly shown in the calculate A_r as shown in Fig. 5c. Nevertheless, the trend of the variation of A_r is captured to a good agreement with the field test.

Case II: Beskos et al. [4]

Beskos et al. [23] proposed a numerical solution based on the boundary element method to solve the problem of vibration screening using open and infilled trenches under plain strain condition. The soil was considered to be linear elastic and homogeneous. To validate his formulation, Beskos et al. [23] solved a passive isolation case using the proposed boundary element formulation. The normalized open trench depth, width and distance from the source of vibration to the trench are $1\lambda_R$, $0.1\lambda_R$ and $5\lambda_R$. The vibration source was considered as a sinusoidal harmonic load with a dynamic load amplitude (P_o) of 1 kN and a frequency of

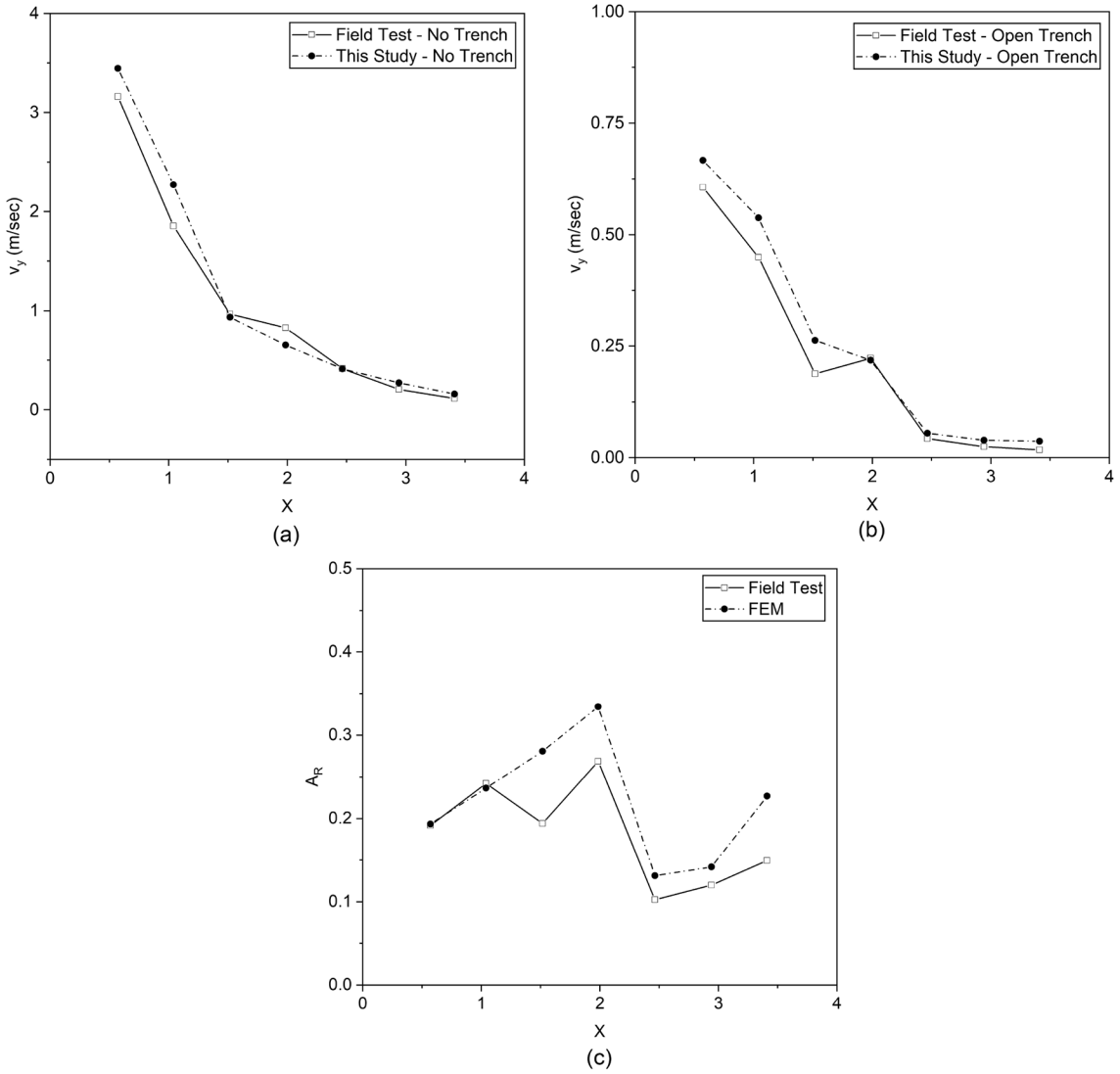

Fig. 5 Comparison between the field and FEM for: **a** Maximum vertical velocities for no trench, **b** maximum vertical velocities for open trench and **c** amplitude reduction ratio

31 Hz. material. The soil the unit weight (γ), Poisson's ratio (ν), soil damping (ξ) and shear wave velocity (V_s) are 18 kN/m^3, 0.25, 5% and 101 m/s, respectively. Furthermore, the Rayleigh wave velocity (V_R) and Rayleigh wavelength (λ_R) are 93 m/s and 3 m, respectively. Figure 6 shows a very good agreement between the results of Beskos et al. [23] and the developed FEM herein.

Parametric Study

The effect of burial depth and buried trench depth is investigated in the conducted parametric study to investigate their effects on the performance of the considered barrier systems. Understanding the consequences of burial depth in reducing the effectiveness of such barriers are of a paramount importance for their design. Furthermore, in buried or open trenches, the trench depth is a critical factor in determining the performance of the wave barriers. Thus, the considered buried depth levels are $0.025\lambda_R$, $0.05\lambda_R$, $0.1\lambda_R$, $0.2\lambda_R$, $0.3\lambda_R$ and $0.4\lambda_R$. While, the considered depths of buried and open trenches are $0.15\lambda_R$, $0.25\lambda_R$, $0.35\lambda_R$ and $0.45\lambda_R$. Furthermore, the type of infilled material was also varied to investigate the performance of soft and rigid infill materials on the performance of buried trenches. Three materials were mainly considered in this study due to their frequent use in the literature which are EPS29 geofoam, concrete and Tire Derived Aggregates (TDA). TDA has been proven to be beneficial for mitigating liquefaction effects and for dampening vibration applications, [24]. All infilled materials were modeled using linear elastic material models and their material properties are presented in Table 2. The impedance ratio (IR) is also shown in Table 2 because the efficiency of trenches is related to the impedance mismatch between the soil and infilled trench material, Yarmohammadi et al. [15]. IR is given by the following equation:

$$\mathrm{IR} = \frac{\rho_{\mathrm{trench}} \times v_{s_{\mathrm{trench}}}}{\rho_{\mathrm{soil}} \times v_{s_{\mathrm{soil}}}}, \tag{9}$$

where ρ is the density and v_s is the shear wave velocity.

Moreover, two special cases were investigated to improve the performance of buried trenches. The first special case is a trapezoidal-shaped buried trench and the inclination of trench walls varied from 4° to 16°. The second special case is a dual buried trench barriers where the spacing between the two trenches varied from 0.1 to $0.2\lambda_R$.

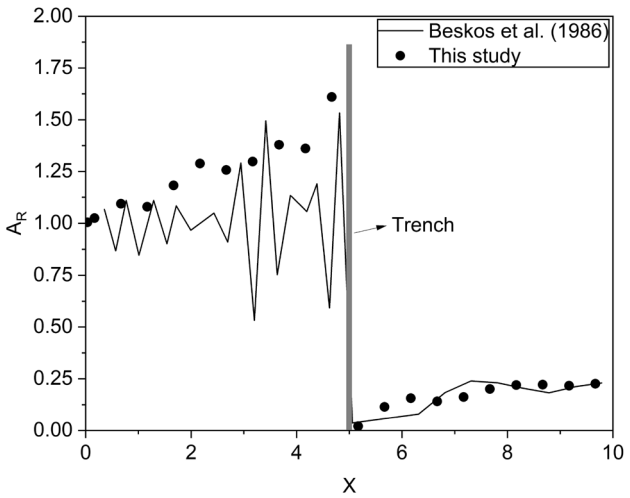

Fig. 6 Comparative study with Beskos et al. [23]

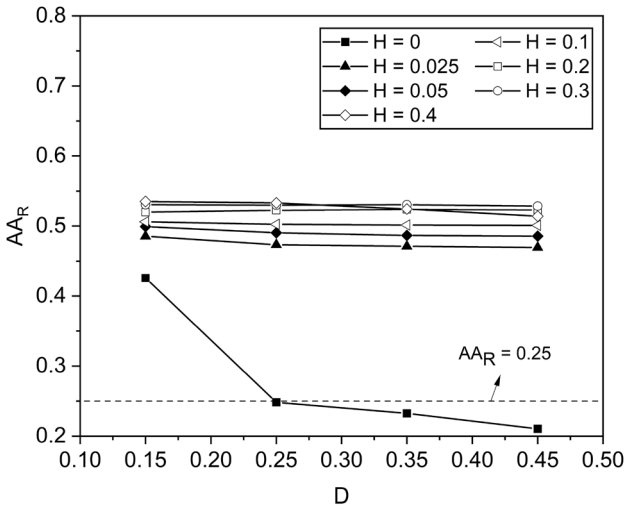

Fig. 7 Influence of trench depth

Table 2 Material properties of the buried trenches infilled material

Material	Unit weight (γ)	Elastic modulus (E)	Poisson's ratio (ν)	Shear wave velocity (V_s)	Damping (ξ)	IR
Geofoam EPS29	0.28 kN/m^3	9.8 MPa	0.16	381 m/s	5%	0.07
Concrete	23.5 kN/m^3	25 GPa	0.15	2130 m/s	5%	0.068
TDA	5.9 kN/m^3	0.51 MPa	0.3	18 m/s	5%	32.27

Effect of Trench Depth

Figure 7 shows the effect of trench depth on the AA_R for various burial depths. Only geofoam-infilled trenches were considered in investigating the trench depth effect. It could be noticed that the open trench (i.e., $H=0$) is significantly influenced by trench depth. In the case of open trench, increasing the normalized trench depth (D) from 0.15 to 0.45 leads to a reduction in AA_R value by about 49%. Furthermore, it was recommended by Woods [5] that an effective trench barrier has an AA_R smaller or equal to 0.25. In this study, the open trench achieved this value by just increasing the trench depth from 0.15 to $0.25\lambda_R$, as shown in Fig. 7. Nevertheless, the influence of barrier depth on the buried trenches is insignificant. In general, the performance of buried trenches is much lower than open trenches. For example, at $D=0.25$, increasing the normalized burial depth to as little as 0.025, the AA_R is increased by about 218% compared to the open trench case. Moreover, as the burial depth increases, the AA_R increases as well. This increase is insignificant when H is larger or equal to 0.2. The reason behind the absence of any influence of the depth on the vibration screening of buried trench barriers could be explained by Fig. 8. According to Fig. 8, the Rayleigh waves are propagating along a soil layer with a thickness of one wavelength, i.e., $1.0\lambda_R$, from the ground surface, Athanasopoulos et al. [25]. Since the maximum considered trench depth is $0.45\lambda_R$, the influence of the vertical component is expected to be extended well beyond the trench depth. Thus, beyond the trench depth, the non-reflected Rayleigh waves will continue to propagate through the soil medium. Additionally, in the case of buried trenches, the overlying soil layer above the trench will further facilitate the propagating of Rayleigh waves beyond the trench barrier. Consequently, the performance of buried trenches is significantly weakened. Also, as shown in Fig. 8, the peak amplitude of the vertical component of Rayleigh waves is occurring at a depth between 0.1 and $0.3\lambda_R$. Hence, the effect of burial depth at H larger or equal to 0.3 is negligible.

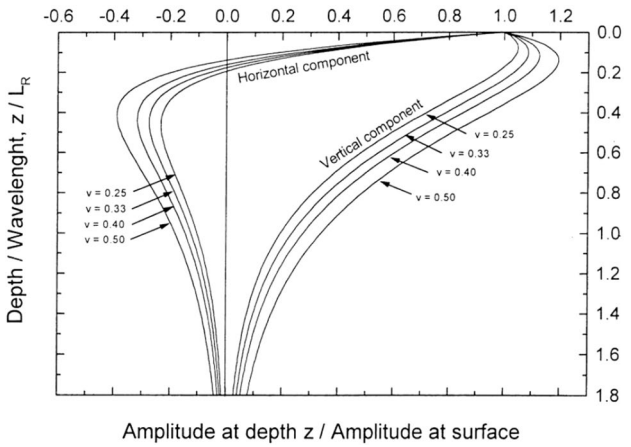

Fig. 8 The decay of the horizontal and vertical components of Rayleigh waves with depth. Adapted from Athanasopoulos et al. [25]

The aforementioned explanation is numerically illustrated by creating a model with an infilled trench depth equal to one wavelength starting from the ground surface. Then, the contour maps of maximum vertical velocity are compared with the finite element model of $D=0.45$ and $H=0.3$ case. As expected, the highest vertical velocity is developed in the vicinity of the load application. As shown in Fig. 9a, the Rayleigh wave could easily pass through the overlaying soil layer above the trench which leads to high intensity of vertical velocity. Additionally, since the trench depth is less than $1.0\lambda_R$, Rayleigh wave velocities with lower intensity are propagating beyond the trench depth. Contrarily, as shown in Fig. 9b, a trench with a depth of $1.0\lambda_R$ is capable of limiting the transmitted waves behind the barrier. However, practically, constructing deep trenches may not be a visible solution due to soil condition or space limitation. Since the wavelength could play an important role in the performance of buried trenches and it is directly related to the applied frequency, investigating the frequency effect on the performance of buried trench is importance. Hence, it is discussed in the following section.

Frequency Effect

The frequency of the vibration source was varied to highlight the effect of the wavelength, as indicated in the previous section, on the performance of buried trenches. The considered vibration source frequencies were 10, 20 and 40 Hz; hence, their corresponding Rayleigh wavelength is 7.8, 3.9 and 1.95 m, respectively. The minimum mesh size of the developed FE models for the 20 and 40 Hz was less than 0.48 and 0.24 m (i.e., less than $\frac{1}{8}\lambda_R$), respectively. The use of normalized dimensions of the burial height (h) and trench depth was avoided herein to emphasize on the significance of frequency effect. Thus, the considered burial heights varied from 0.20 to 3.10 m. Furthermore, the trench depth was 3.50 m. It could be seen from Fig. 10 that the frequency significantly influences the performance of the geofoam-infilled buried trenches. As expected, as the Rayleigh wavelength increases, the performance of buried trenches degrades. In addition, at a lower burial depth and at higher frequencies, the buried trenches could achieve significant vibration screening performance, i.e., AA_R is around 0.25. This could be explained by Fig. 8, as discussed before, where more propagated waves could be diffracted away from the ground surface, especially when the Rayleigh wavelength is lower. The influence of the Rayleigh wavelength could be clearly illustrated by Fig. 11. It could be concluded from Fig. 11a that the surface displacements are remarkably evident at lower frequency due

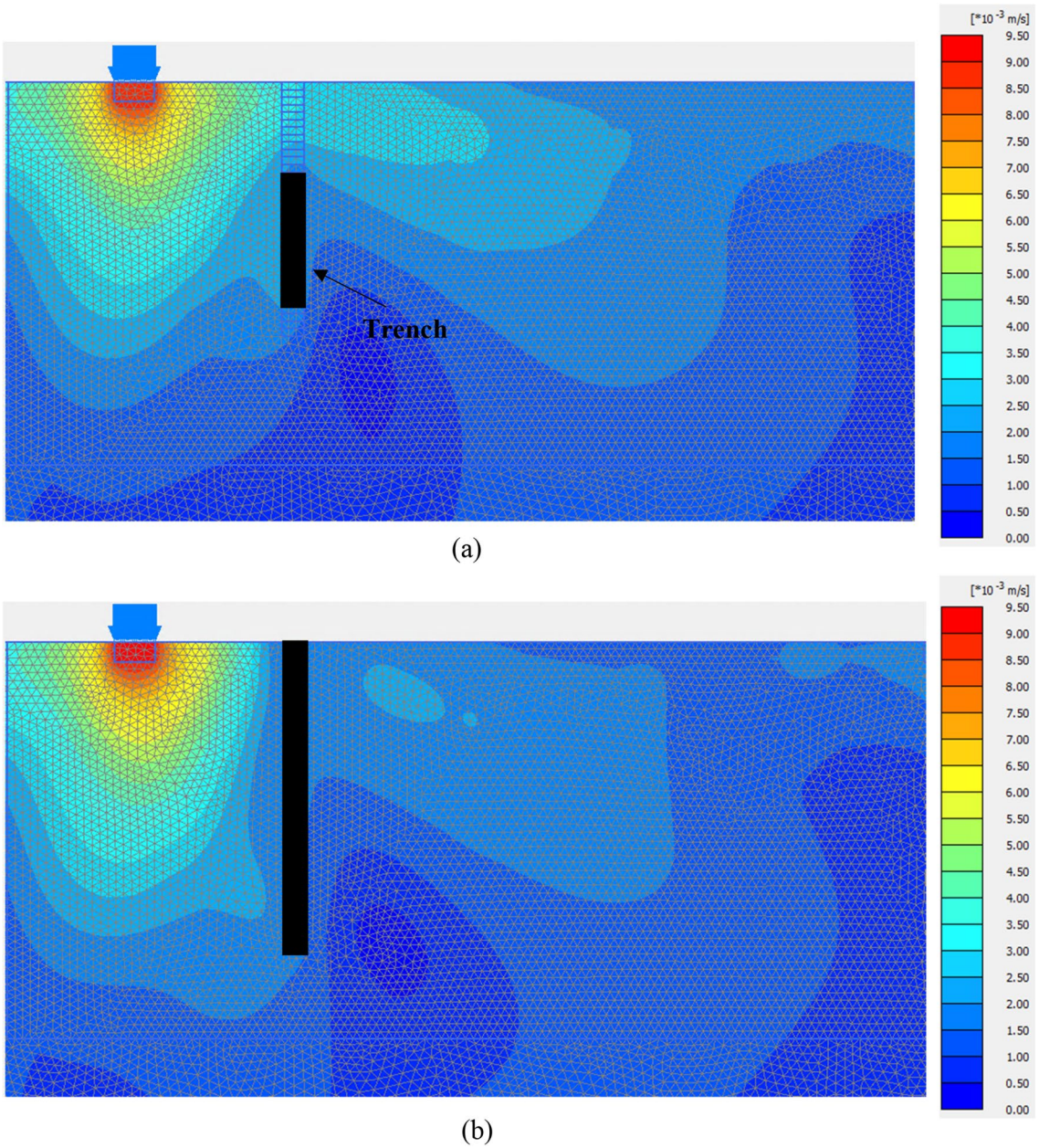

Fig. 9 Influence of Rayleigh waves with depth: **a** $D=0.45$ and $H=0.3$; **b** $D=1$ and $H=0$

to the propagated waves through the overlying soil above trench as well as underneath the trench. Nevertheless, at higher frequencies, the influence of Rayleigh waves with depth is decreased; thus, the buried trenches reduced surface displacements by diffracting more waves away from the ground surface.

Effect of Infill Material

Figure 12 shows the variation of AA_R with the normalized burial depth for various infill materials. In general, each of the considered infill material is not sufficient enough to improve the vibration screening capability of the buried trenches. Nevertheless, TDA-infilled buried trenches have a very reasonable AA_R up to a normalized burial depth of 0.05 which is could be comparable with open trenches. It is noteworthy that the field test results conducted by Jafari [26] on linear, semi-circular and circular open and TDA-infilled trenches showed that TDA-infilled trenches are as effective as open trenches in attenuating vibrations. However, in the case of buried trenches, as the normalized burial depth exceeds 0.1, the performance of TDA-infilled buried

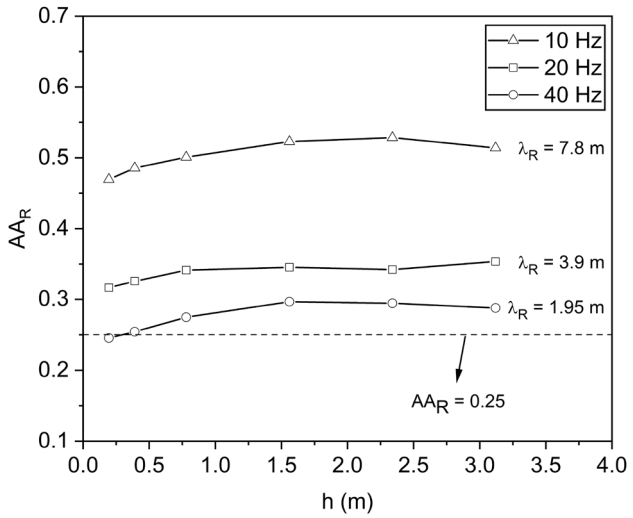

Fig. 10 Influence of the source frequency on the performance of buried trenches

trenches drops significantly. Furthermore, the geofoam buried trenches provided a better vibration screening than the concrete buried trenches up to a normalized depth of 0.1. Celebi et al. [27] also concluded that using softer infilled material increased the effectiveness of the infilled trench based on a series of field tests. It could also be noted that at H larger or equal to 0.2, the type of infilled material does not play an important role in screening ground-borne vibrations.

Special Cases

This section discusses the use of dual trenches and a trapezoidal-shaped trenches to improve the effectiveness of buried trenches. As shown in Fig. 13, the normalized burial depth and the normalized trench depth are equal to 0.1 and 0.45, respectively. The trench infilled material considered is TDA only. Moreover, in the case of dual trenches, the distance between the buried trenches (S) is varied from 0.1 to $0.2\lambda_R$ to investigate its effect on the performance of dual

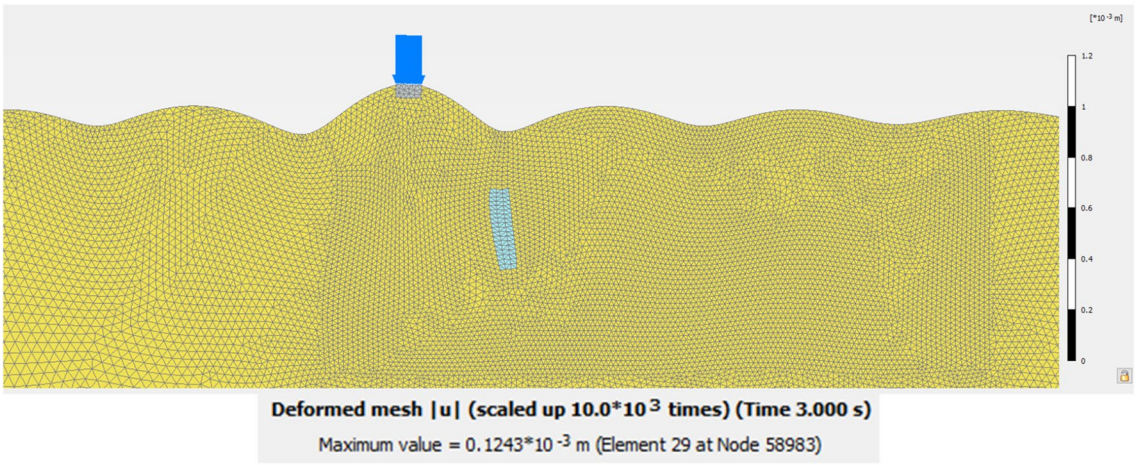

(a)

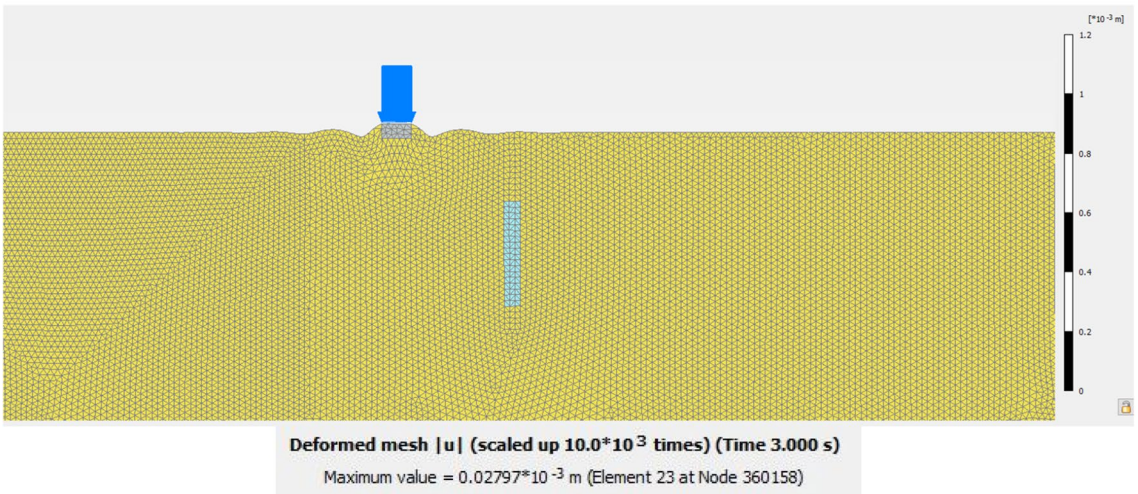

(b)

Fig. 11 Deformed mesh at $h = 2.34$ m for the **a** 10 Hz model and **b** 40 Hz model

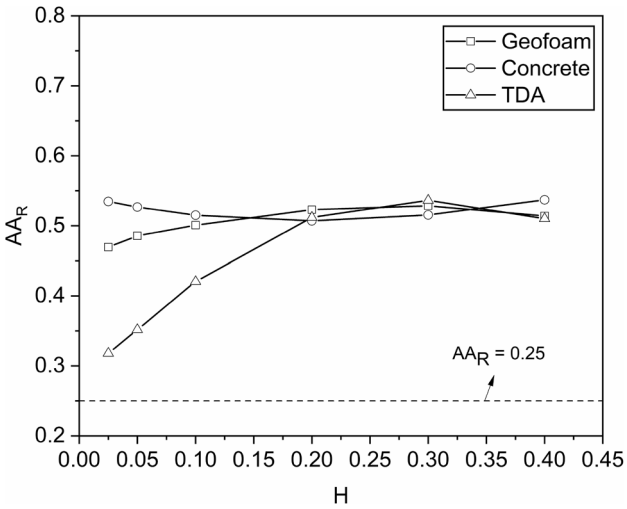

Fig. 12 variation of AAR with the normalized burial depth for various infill materials

trenches. Moreover, as shown in Table 3, three cases were considered for the trapezoidal-shaped buried trench. The area of the trapezoidal trench in case 1 is the same as the area of a single rectangular trench used in the previous sections. This case is mainly considered to compare the shape effect only without impacting the amount of infilled material. Furthermore, the inclination of the trapezoidal trench walls (δ) is increased to evaluate its impact on the AA_R of the trapezoidal buried trenches.

As shown in Fig. 14, case I slightly improved the effectiveness of the buried trench compared to the rectangular single trench. On the other hand, case II and III reduced the AA_R considerably by around 35% and 48%, respectively. It is very important to note that with just an inclination of 16°, the buried trench is now considered an effective barrier since its AA_R is less than 0.25.

Figure 15 shows the AA_R for a single rectangular trench and dual trenches. The dual trench results show

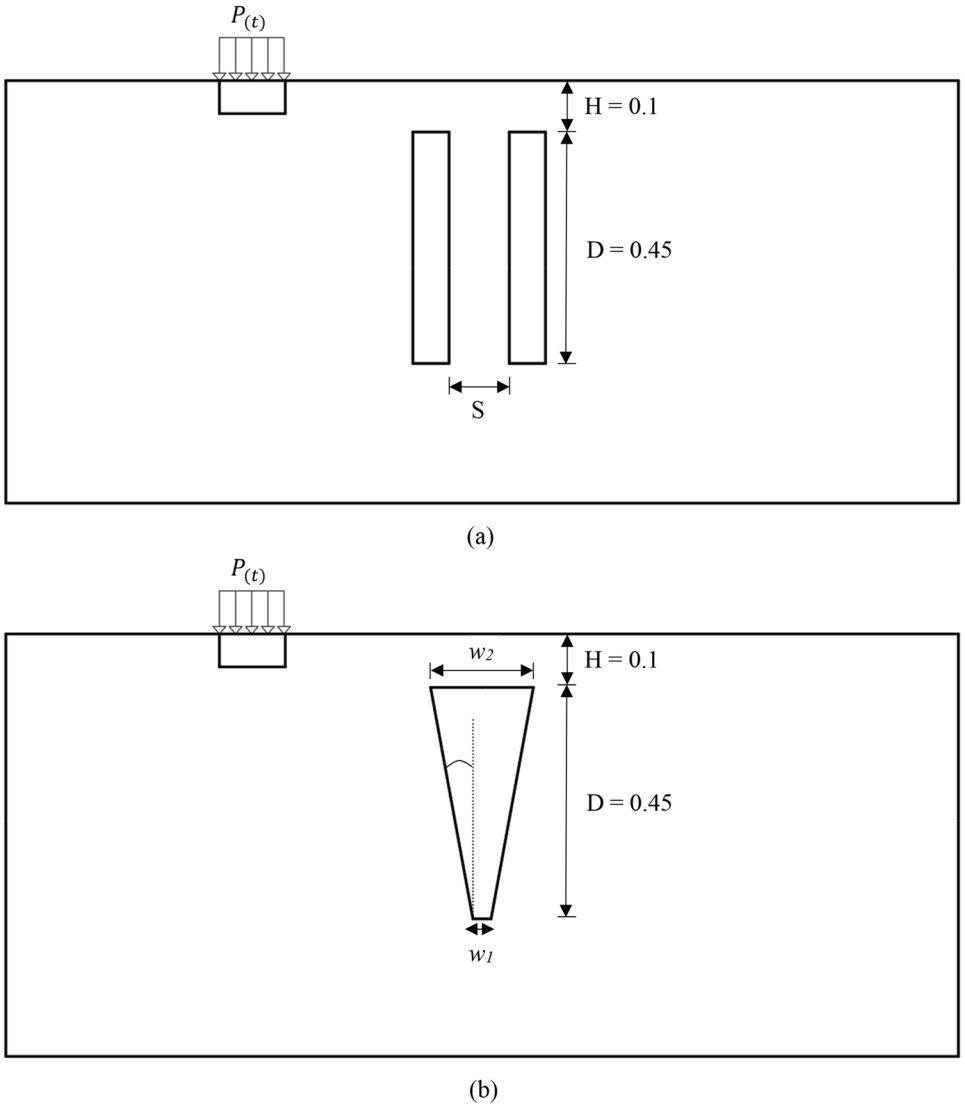

Fig. 13 A schematic diagram for: **a** dual buried trench; **b** trapezoidal buried trench

Table 3 Dimensions of the trapezoidal-shaped buried trench

Case #	w_1 (m)	w_2 (m)	δ (°)
I	0.275	0.825	4
II	0.275	1.56	10
III	0.275	2.34	16

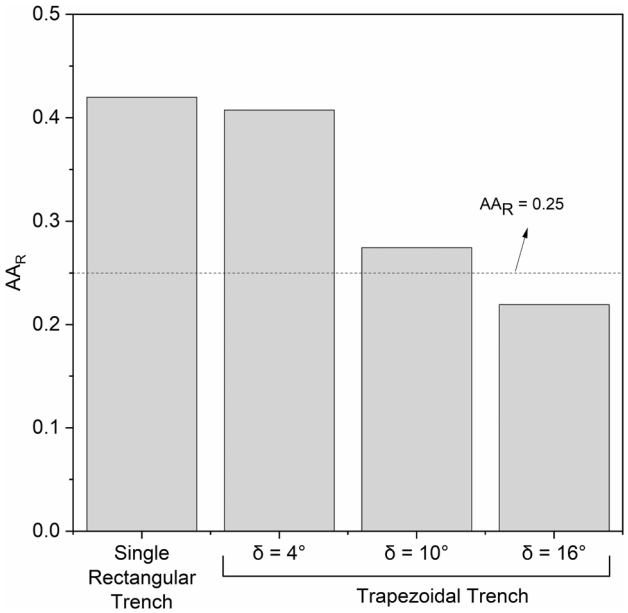

Fig. 14 Performance of trapezoidal buried trench

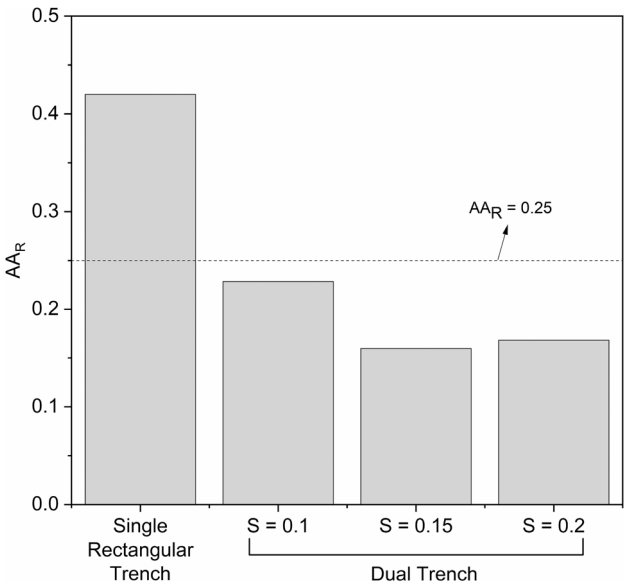

Fig. 15 Performance of dual buried trench

that regardless of the space between the trenches, all dual trenches are considered effective. It could be concluded that the dual trenches could significantly improve the vibration screening of infilled buried trenches.

Conclusions

A 2D plain strain FEM was developed to investigate the performance of buried trenches. The model was validated against the results of a field test and a numerical study. Furthermore, a parametric study was conducted to investigate various key factors, i.e., trench depth, burial depth and infilled material type, on the effectiveness of buried trench wave barriers. Based on the conducted parametric study, the following conclusions are made:

- The effectiveness on trench barriers drops significantly with increasing burial depth by as low as $0.025\lambda_R$.
- The influence of Rayleigh wave with depth especially at low to low intermediate (i.e., < 15 Hz) could affect negatively the effectiveness of single buried trenches. A greater Rayleigh wavelength will diminish the influence of the buried trench depth decreases.
- The TDA-buried infill trenches had the best performance comparing to the geofoam- and concrete-infilled buried trenches. However, this superiority is limited to a burial depth less than or equal to $0.1\lambda_R$.
- A trapezoidal-shaped buried trench proved to have a better performance than a single rectangular trench. This improvement is more significant when the inclination angle is larger than 10°.
- Dual buried trenches have a great impact on decreasing the A_R compared to the signal rectangular trench. Regardless of the distance between the two trenches in a dual trench system, the A_R dropped below 0.25. Thus, the dual trench system could effectively overcome the limitation of the buried trenches.

Acknowledgments The authors acknowledge the funding provided by the Natural Sciences and Engineering Research Council of Canada (NSERC) and Divert NS for this research project.

References

1. Saikia A (1984) (2014) Numerical study on screening of surface waves using a pair of softer backfilled trenches. Soil dynamics and earthquake engineering 65:206–213. https://doi.org/10.1016/j.soildyn.2014.05.012
2. Mahdavisefat E, Heshmati A, Salehzadeh H, Bahmani H, Sabermahani M (2017) Vibration screening by trench barriers, a

review. Arab J Geosci 10(23):1–14. https://doi.org/10.1007/s12517-017-3279-3
3. Henwood JT, Haramy KY Vibrations induced by construction traffic: a historic case study. In: Geophysics 2002. The 2nd Annual Conference on the Application of Geophysical and NDT Methodologies to Transportation Facilities and InfrastructureFederal Highway Administration (FHWA-WRC-02–001), Transportation Research Board, California Department of Transportation, 2002.
4. Barkan DD (1962) Dynamics of bases and foundations. McGraw-Hill, New York
5. Woods RD (1968) Screening of surface waves in soils. J Soil Mech Found Div ASCE 94(4):951–979
6. Jesmani M, Shafie MR, SadeghiVileh R (2008) Finite element analysis of active isolation of deep foundation in clayey soil by rectangular trenches. Electron J Geotech Eng 13(E):143–152
7. Çelebi E, Kırtel O (2013) Non-linear 2-D FE modeling for prediction of screening performance of thin-walled trench barriers in mitigation of train-induced ground vibrations. Constr Build Mater 42:122–131. https://doi.org/10.1016/j.conbuildmat.2012.12.071
8. Murillo C, Thorel L, Caicedo B (2009) Ground vibration isolation with geofoam barriers: centrifuge modeling. Geotext Geomembr 27(6):423–434. https://doi.org/10.1016/j.geotexmem.2009.03.006
9. Orehov V, Moghanlou RN, Negahdar H, Varagh AMB (2012) Investigation effects of trench barrier on the reducing energy of surface waves in soils. In: 15th World Conference on Earthquake Engineering, 2012. pp 24–28
10. Haupt W (1977) Isolation of vibrations by concrete core walls. In: Proceedings of the ninth international conference on soil mechanics and foundation engineering, pp 251–256
11. Haupt WA (1978) Numerical methods for the computation of steady-state harmonic wave fields. Dyn Methods Soil Rock Mech 1:255–280
12. Haupt WA (1978) Surface waves in nonhomogeneous half-space. Dyn Methods Soil Rock Mech 1:335–367
13. Naggar MHE, Chehab AG (2005) Vibration barriers for shock-producing equipment. Can Geotech J 42(1):297–306. https://doi.org/10.1139/t04-067
14. Zoccali P, Cantisani G, Loprencipe G (2015) Ground-vibrations induced by trains: Filled trenches mitigation capacity and length influence. Constr Build Mater 74:1–8. https://doi.org/10.1016/j.conbuildmat.2014.09.083
15. Yarmohammadi F, Rafiee-Dehkharghani R, Behnia C (1984) Aref AJ (2019) Design of wave barriers for mitigation of train–induced vibrations using a coupled genetic-algorithm/finite-element methodology. Soil Dyn Earthq Eng 121:262–275. https://doi.org/10.1016/j.soildyn.2019.03.007
16. Yarmohammadi F, Rafiee-Dehkharghani R (2020) An optimal design procedure of wave barriers for mitigation of underground and above-ground railway vibrations. Int J Struct Stabil Dyn 20(11):2050121
17. Feng S, Li J, Zhang X, Chen Z, Zheng Q, Zhang D (2019) Numerical analysis of buried trench in screening surface vibration. Soil Dyn Earthq Eng 1984:126. https://doi.org/10.1016/j.soildyn.2019.105822
18. Kramer SL (1996) Geotechnical earthquake engineering. Pearson Education India, Chennai
19. Lysmer J, Kuhlemeyer RL (1969) Finite dynamic model for infinite media. J Eng Mech Div 95(4):859–878
20. Brinkgreve RBJ, Vermeer PA (1998) PLAXIS finite element code for soil and rock analysis. A.A. Balkema Publishers, Delft
21. Wang JG, Sun W, Anand S (2009) Numerical investigation on active isolation of ground shock by soft porous layers. J Sound Vib 321(3–5):492–509. https://doi.org/10.1016/j.jsv.2008.09.047
22. Alzawi A (1984) Hesham El Naggar M (2011) Full scale experimental study on vibration scattering using open and in-filled (GeoFoam) wave barriers. Soil Dyn Earthq Eng 31(3):306–317. https://doi.org/10.1016/j.soildyn.2010.08.010
23. Beskos D, Dasgupta B, Vardoulakis I (1986) Vibration isolation using open or filled trenches. Solids Fluids Struct Fluid-Struct Interact Biomech Micromech Multisc Mech Materi Const Model Nonlinear Mech Aerodyn 1(1):43–63. https://doi.org/10.1007/BF00298637
24. Moussa A, and El Naggar H (2020) Dynamic characterization of tire derived aggregates. J Mater Civ Eng. https://doi.org/10.1061/(ASCE)MT.1943-5533.0003583
25. Athanasopoulos G, Pelekis P, Anagnostopoulos G (2000) Effect of soil stiffness in the attenuation of Rayleigh-wave motions from field measurements. Soil Dyn Earthq Eng 19(4):277–288
26. Jafari F (2016) Beneficial use of recycled scrap tire shreds to isolate ground-borne vibrations. Rutgers University-Graduate School-New Brunswick, New Brunswick
27. Çelebi E, Fırat S, Beyhan G, Çankaya İ, Vural İ (1984) Kırtel O (2009) Field experiments on wave propagation and vibration isolation by using wave barriers. Soil Dyn Earthq Eng 29(5):824–833. https://doi.org/10.1016/j.soildyn.2008.08.007